Implementation of a new memristor-based multiscroll hyperchaotic system

Article *in* Pramana · February 2017

DOI: 10.1007/s12043-016-1342-3

3 authors, including:

Chunhua Wang
Hunan University
167 PUBLICATIONS **792** CITATIONS
SEE PROFILE

Ling Zhou
Hunan University
9 PUBLICATIONS **62** CITATIONS
SEE PROFILE

Pramana – J. Phys. (2017) 88: 34
DOI 10.1007/s12043-016-1342-3

Implementation of a new memristor-based multiscroll hyperchaotic system

CHUNHUA WANG, HU XIA* and LING ZHOU

College of Computer Science and Electronic Engineering, Hunan University, Changsha, 410082, China
*Corresponding author. E-mail: 853200447@qq.com

MS received 14 December 2015; revised 23 June 2016; accepted 29 July 2016; published online 17 January 2017

Abstract. In this paper, a new type of flux-controlled memristor model with fifth-order flux polynomials is presented. An equivalent circuit which realizes the action of higher-order flux-controlled memristor is also proposed. We use the memristor model to establish a memristor-based four-dimensional (4D) chaotic system, which can generate three-scroll chaotic attractor. By adjusting the system parameters, the proposed chaotic system performs hyperchaos. Phase portraits, Lyapunov exponents, bifurcation diagram, equilibrium points and stability analysis have been used to research the basic dynamics of this chaotic system. The consistency of circuit implementation and numerical simulation verifies the effectiveness of the system design.

Keywords. Memristor; hyperchaos; three-scroll chaotic attractor; circuit implementation.

PACS Nos 05.40.Jc; 05.45.Pq

1. Introduction

Leon Chua proposed the concept of memristor as the fourth circuit element in 1971 [1]. It represents a relationship between the flux and the charge. Memristor is a two-terminal element with variable resistance called memristance which depends on how much electric charge has been passed through it in a particular direction. In 2008, researchers in Hewlett–Packard announced that a solid-state implementation of memristor has been successfully fabricated [2]. Since then, memristor-based chaotic systems gained a lot of attention. Researchers mainly focussed on using a memristor to substitute Chua's diode of Chua's circuit [3–12], building various chaotic circuits based on memristor and then completing the analysis of dynamics. In addition, Li [13] proposed a memristor oscillator based on a twin-T network. Through coupling, Corinto [14] realized a chaotic oscillator containing three flux-controlled memristor. Based on a nonlinear model of HP TiO_2 memristor, two different memristor-based chaotic circuits are constructed [15,16]. In the past few years, many researchers devoted themselves to introducing the memristor to Lü, Chen and Lorenz chaotic systems [17,18], and then nonlinear systems are further studied using topological horseshoe theory.

So far, memristor-based chaotic systems are limited to single-scroll and double-scroll, and so chaotic dynamics was not complicated. Memristor-based multiscroll chaotic systems have been rarely found. In 2014, Li [19] presented a memristor-based three-scroll chaotic system. However, Li [19] used the additional ordinary nonlinear function to generate a three-scroll attractor. So the circuit is more complicated and the system is not a memristor-based multiscroll chaotic system in the real sense. In 2014, Teng [20] used memristor to achieve multiscroll chaotic attractor, without the additional ordinary nonlinear function. A fifth-order generalized charge-controlled memristor is presented in [20] and multiscroll chaotic system is implemented. However, only two-scroll and four-scroll chaotic systems are obtained in [20], and then odd-scroll could not be achieved. Moreover, charge-controlled memristor was used to implement chaotic system in [20], and then charge-controlled memristor emulator is complicated and has difficulty in circuit implementation. Furthermore, memristor and memristor-based chaotic system in [20] are realized using mathematical simulation only, without circuit implementation.

Based on the above theory, this paper proposes a new type of flux-controlled memristor model with fifth-order flux polynomials, and the memristor model is

used in a four-dimensional (4D) chaotic system, which can generate chaotic phenomenon. We use higher-degree polynomial memductance function to increase complexity of the chaos. So the chaotic system can generate a three-scroll chaotic attractor. The memristor model is simulated by circuit simulation. On this basis, memristor-based chaotic system is also implemented by circuit simulation. In this paper, we propose the memristor model to establish a memristor-based four-dimensional multiscroll attractor, while Teng [20] modelled three-dimensional multiscroll attractor.

The rest of this paper is organized as follows: In §2, the memristor theory is presented and then a new memristor emulator circuit is proposed. In §3, the chaotic system equations and dynamical characteristics are described. In §4, the chaotic circuit and multisim simulation results are presented. In §5, the conclusion is presented.

2. Memristor system

2.1 *Memristor model*

Memristor is a new passive two-terminal circuit element in which there is a functional relationship between charge q and magnetic flux φ. The memristor is governed by the following relation:

$$\begin{cases} v = M(q)i \\ i = W(\varphi)v \end{cases}, \tag{1}$$

where the two nonlinear functions $M(q)$ and $W(\varphi)$, called the memristance and memductance, respectively, are defined by

$$\begin{cases} W(\varphi) = \dfrac{\mathrm{d}q(\varphi)}{\mathrm{d}\varphi} \\ M(q) = \dfrac{\mathrm{d}\varphi(q)}{\mathrm{d}q} \end{cases}. \tag{2}$$

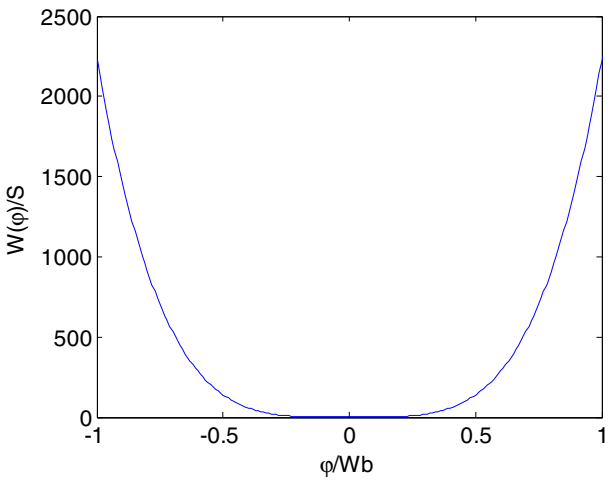

Figure 1. The relationship curve between φ and $W(\varphi)$.

In this paper, we assume that the definition of memristor is a smooth and nonlinear function, which is defined as

$$q(\varphi) = a\varphi^5 + b\varphi^3 + c\varphi + d. \tag{3}$$

From eq. (3), memductance $W(\varphi)$ is given by

$$W(\varphi) = 5a\varphi^4 + 3b\varphi^2 + c. \tag{4}$$

When $5a = 2227\ \mathrm{S/Wb^4}$, $3b = -1.087\ \mathrm{S/Wb^2}$, $c = 0.135$ mS, then $W(\varphi)$ can be given by

$$W(\varphi) = (2227\ \mathrm{S/Wb^4})\varphi^4 - (1.087\ \mathrm{S/Wb^2})\varphi^2 + (0.135\ \mathrm{mS}). \tag{5}$$

The relationship curve between φ and $W(\varphi)$ is shown in figure 1.

2.2 *Memristor emulator circuit*

On the basis of memristor theory, we propose a circuit to emulate the behaviour of the memristor. The schematic is depicted in figure 2.

The schematic is composed of two operational amplifiers, four multipliers, one capacitor and four resistances. The first-level operational amplifier U1 is used to avoid load effect. The second-level operational amplifier U2, resistance R_0 and capacitor C_0 together form the integral circuit, used to implement integral function:

$$v_a(t) = -\frac{1}{R_0C_0}\int_{-\infty}^{t} v(\tau)\,\mathrm{d}\tau = -\frac{1}{R_0C_0}\varphi(t). \tag{6}$$

According to the input-to-output function of G1–G4 (AD633), $v_b(t)$ and $v_d(t)$ can be calculated using the equations

$$v_b(t) = -g_1g_2[v_a(t)]^2v(t)\,, \tag{7}$$

$$v_d(t) = g_1^2g_3g_4[v_a(t)]^4v(t). \tag{8}$$

As shown in eqs (7) and (8), coefficients g_1, g_2, g_3 and g_4 are the scaling factors of multipliers G1, G2, G3 and

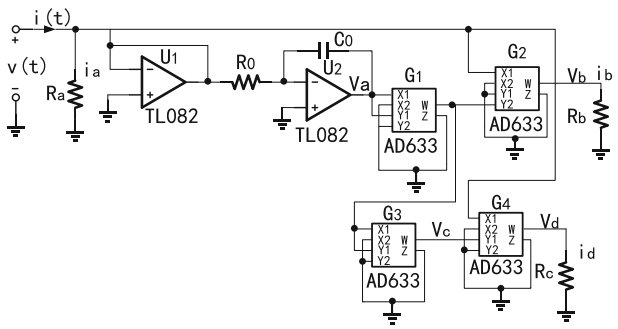

Figure 2. Schematic for realizing a memristor.

G4. Therefore, the current going through the emulator can be rewritten as

$$i(t) = \frac{v(t)}{R_a} + \frac{v_b(t)}{R_b} + \frac{v_d(t)}{R_c}. \quad (9)$$

By combining eqs (6)–(9), the flux-controlled memductance can be calculated as

$$W(\varphi) = \frac{1}{R_a} - \frac{g_1 g_2}{R_b (R_0 C_0)^2}\varphi^2 + \frac{g_1^2 g_3 g_4}{R_c (R_0 C_0)^4}\varphi^4. \quad (10)$$

Let $R_a = 7.4\ \text{k}\Omega$, $R_b = 92\ \Omega$, $R_c = 4.4\ \Omega$, $R_0 = 100\ \text{k}\Omega$, $C_0 = 100\ \text{nF}$ and $g_1 = g_2 = g_3 = g_4 = 0.1\ \text{V}^{-1}$. We obtain the flux-controlled memductance corresponding to eq. (5). Here $t_0 = R_0 C_0$ is the time that determines the pace of the integration. t_0 and f_0 provide the natural time and frequency scales for the memristive circuit (the preceding parameters imply $t_0 \sim 0.01$ s and $f_0 \sim 100$ Hz).

In order to validate that the memristor model which we propose in this article have real memristor characteristics, we have done a multisim simulation to obtain diverse i–v characteristics by choosing appropriate functional forms of $v_i(t)$. Figure 3 shows the i–v curves when $v_i(t) = v_0 \sin(2\pi f t)$ for $f = f_0$, $f = 4f_0$ and $f = 10f_0$. When $f \leq 10f_0$, a pinched hysteresis loop is found in the i–v curve. By increasing the frequency, the pinched hysteresis loop gradually contracts. When $f > 10f_0$, the pinched hysteresis loop contracts to a single-valued function. Here we cannot directly measure current in the multisim simulation. So we convert the current i into the corresponding voltage v_p by using AD844. The converting resistor $R_p = 10\ \text{k}\Omega$ and the converting voltage $v_p = i \cdot R_p$. So we can conclude that the proposed memrsitor model satisfies the pinched hysteresis characteristic of the memrsitor [1,2,21].

3. Chaotic system

In order to further study the effectiveness of the proposed memristor model, this section introduces the use of memristors within fourth-order differential equations aiming at the generation of chaotic attractors.

3.1 *System equations and phase portraits*

The proposed dimensionless chaotic system is as follows:

$$\begin{cases} \dfrac{\mathrm{d}x}{\mathrm{d}t} = \alpha(y + x - W(w)x), \\ \dfrac{\mathrm{d}y}{\mathrm{d}t} = \beta x + \gamma y - z, \\ \dfrac{\mathrm{d}z}{\mathrm{d}t} = \delta y - z, \\ \dfrac{\mathrm{d}w}{\mathrm{d}t} = x, \end{cases} \quad (11)$$

where x, y, z and w are the states of the chaotic system and α, β, γ and δ are the parameters. If v_x, v_y, v_z indicate voltages and φ indicates the magnetic flux, then eq. (12) can be easily achieved with an analog circuit, as shown in figure 4. Therefore, the state equation of the memristive chaotic circuit is

$$\begin{cases} C_x \dot{v}_x = v_x/R_1 + v_y/R_2 - v_x W(\varphi), \\ C_y \dot{v}_y = v_x/R_3 + v_y/R_4 - v_z/R_5, \\ C_z \dot{v}_z = v_y/R_7 - v_z/R_6, \\ \dot{\varphi} = v_x. \end{cases} \quad (12)$$

Further, we obtain

$$\begin{cases} C_x \dot{v}_x = v_x/R_1 + v_y/R_2 \\ \quad - v_x\left[\dfrac{1}{R_a} - \dfrac{g_1 g_2}{R_b (R_0 C_0)^2}\varphi^2 + \dfrac{g_1^2 g_3 g_4}{R_c (R_0 C_0)^4}\varphi^4\right], \\ C_y \dot{v}_y = v_x/R_3 + v_y/R_4 - v_z/R_5 \\ C_z \dot{v}_z = v_y/R_7 - v_z/R_6 \\ \dot{\varphi} = v_x. \end{cases} \quad (13)$$

Let $\tau = t \cdot RC$ denotes the physical time, where t is the dimensionless time, $R = 100\ \text{k}\Omega$ is a reference resistor

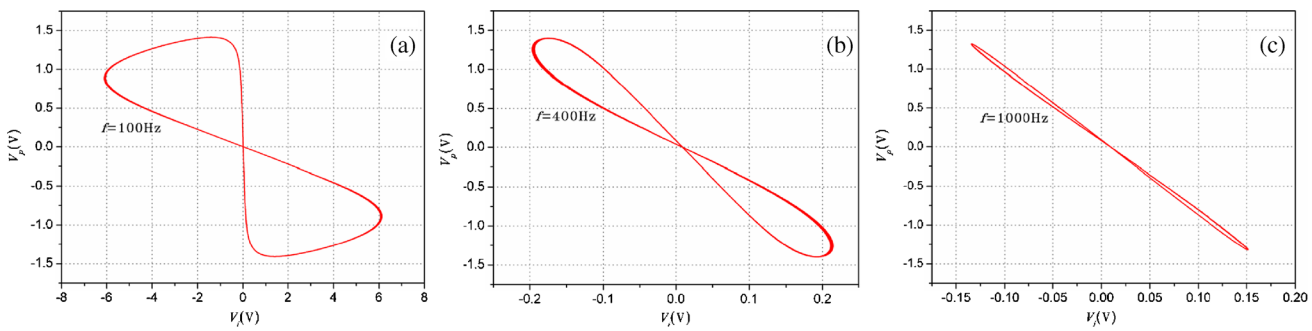

Figure 3. The memristor i–v curves for (**a**) $f = f_0$, (**b**) $f = 4f_0$ and (**c**) $f = 10f_0$.

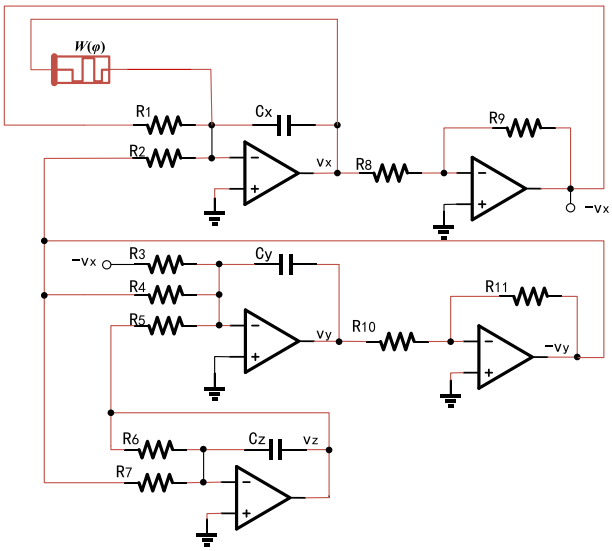

Figure 4. Circuit implementation of the 4D chaotic system with a memristor.

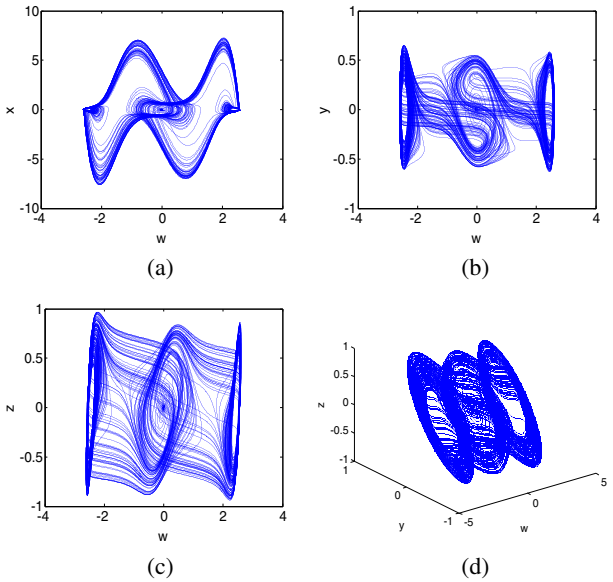

Figure 5. Three-scroll chaotic attractor: (**a**) w–x plane, (**b**) w–y plane, (**c**) w–z plane and (**d**) w–y–z plane.

and C=100 nF is a reference capacitor. Equations (13) can be written as follows:

$$\begin{cases} \dfrac{C_x \mathrm{d}v_x}{C\mathrm{d}t} = \dfrac{v_x R}{R_1} + \dfrac{v_y R}{R_2} \\ \qquad - \alpha v_x \left[\dfrac{R}{\alpha R_a} - \dfrac{R g_1 g_2}{\alpha R_b} \left(\dfrac{\varphi}{R_0 C_0} \right)^2 \right. \\ \qquad \left. + \dfrac{R g_1^2 g_3 g_4}{\alpha R_c} \left(\dfrac{\varphi}{R_0 C_0} \right)^4 \right], \\ \dfrac{C_y \mathrm{d}v_y}{C\mathrm{d}t} = \dfrac{v_x R}{R_3} + \dfrac{v_y R}{R_4} - \dfrac{v_z R}{R_5}, \\ \dfrac{C_z \mathrm{d}v_z}{C\mathrm{d}t} = \dfrac{v_y}{R_7} - \dfrac{v_z}{R_6}, \\ \dfrac{\mathrm{d}}{\mathrm{d}t} \left(\dfrac{\varphi}{RC} \right) = v_x. \end{cases} \tag{14}$$

The parameters of the memristive chaotic circuit can be considered as follows: $C_x = C_y = C_z = C_0 = C$, $R/R_1 = R/R_2 = \alpha$, $R/R_3 = \beta$, $R/R_4 = \gamma$, $R/R_7 = \delta$, $R/R_5 = R/R_6 = R/R_0 = 1$. Let $x = v_x$, $y = v_y$, $z = v_z$, $w = \varphi/R_0 C_0$, then eqs. (14) are equivalent to eq. (11). The function $W(w)$ in eq. (11) represents the dimensionless function of the memristor as follows:

$$W(w) = \frac{R}{\alpha R_a} - \frac{R g_1 g_2}{\alpha R_b} w^2 + \frac{R g_1^2 g_3 g_4}{\alpha R_c} w^4, \tag{15}$$

where $R/\alpha R_a = 1.8$, $R g_1 g_2/\alpha R_b = 1.45$, $R g_1^2 g_3 g_4/\alpha R_c = 0.3$.

Typical α, β, γ and δ values are: $\alpha = 7.5$, $\beta = 0.067$, $\gamma = 1.033$ and $\delta = 2.1$. Choosing the initial conditions $(x_0, y_0, z_0, w_0) = (0, 0, 0.01, 0)$, system (11) has been simulated using the above parameters. The chaotic attractor generated by means of MATLAB simulation is illustrated in figure 5. We can see a three-scroll chaotic attractor which is different from the attractors generated by other memristor-based chaotic systems.

3.2 *Lyapunov exponents and bifurcation diagram*

The Lyapunov exponents and bifurcation diagram are effective approaches for determining whether a system is chaotic. The rate of separation can be different for different orientations of the initial separation vector, and hence the number of Lyapunov exponents is equal to the number of dimensions in phase space. For a four-dimensional autonomous continuous time system, this system will have four Lyapunov exponents. A positive Lyapunov exponent implies an expanding direction in phase space. However, if the sum of Lyapunov exponents is negative, then this system has contracting volumes in phase space. These two seemingly contradictory properties are indications of chaotic behaviour in a dynamical system.

So we provide the corresponding Lyapunov exponent spectrum of system (11), which is shown in figure 6. As the fourth Lyapunov exponent is too large, we only show the first three Lyapunov exponents. In the numerical simulation, only α varies, while the other parameters are fixed at $\beta = 0.067$, $\gamma = 1.033$ and $\delta = 2.1$. Notice that for $\alpha = 7.5$, the corresponding Lyapunov exponents are: $LE_1 = 0.06$, $LE_2 = 0.03$, $LE_3 = 0$, $LE_4 = -12$. There are two positive Lyapunov exponents and the sum of the Lyapunov exponents is negative, indicating hyperchaotic behaviour.

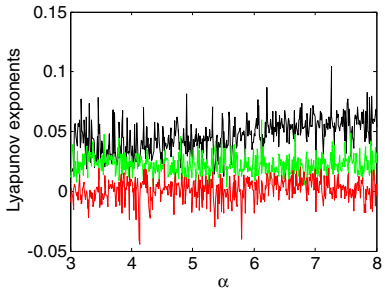

Figure 6. Lyapunov exponent spectrum.

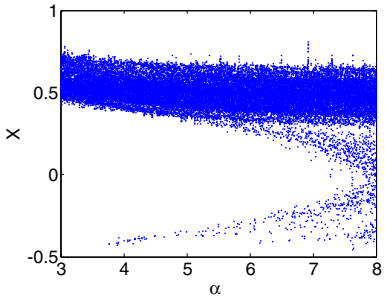

Figure 7. Bifurcation diagram.

Figure 7 shows the bifurcation diagram of system (11) with the same parameters.

3.3 *Equilibrium points and stability analysis*

Let $\dot{x} = \dot{y} = \dot{z} = \dot{w} = 0$, then we can get the equilibrium set of chaotic system (11).

$$P_0 = (x_0, y_0, z_0, w_0) = (0, 0, 0, d). \tag{16}$$

Equation (16) is an equilibrium set of this system. We can see that d is uncertain but constant. We can write the Jacobian matrix of this system at the equilibrium set P_0 as follows:

$$J(p_0) = \begin{bmatrix} \alpha(1 - W(d)) & \alpha & 0 & 0 \\ \beta & \gamma & -1 & 0 \\ 0 & \delta & -1 & 0 \\ 1 & 0 & 0 & 0 \end{bmatrix}. \tag{17}$$

The system characteristic equation can be written as

$$\lambda(\lambda^3 + a_2\lambda^2 + a_1\lambda + a_0) = 0, \tag{18}$$

where

$$\begin{cases} a_0 = \alpha(-1 + W(d))(\delta - \gamma) - \alpha\beta \\ a_1 = \alpha(-1 + W(d))(1 - \gamma) + \delta - \gamma - \alpha\beta. \\ a_2 = \alpha(-1 + W(d)) + 1 - \gamma \end{cases} \tag{19}$$

When $\alpha = 7.5$, $\beta = 0.067$, $\gamma = 1.033$ and $\delta = 2.1$, we can choose a series of typical values of the constant d, and the corresponding characteristic roots are shown in table 1.

Table 1. Different values of d corresponding to the four characteristic roots.

d	λ_1	$\lambda_{2,3}$	λ_4
0	−6.0669	0.0499 ± 0.9848i	0
0.1	−5.9592	0.0504 ± 0.9839i	0
0.2	−5.6391	0.0518 ± 0.9807i	0
0.5	−3.5152	0.0632 ± 0.9443i	0
1	2.8386	-0.0903 ± 1.0750i	0
2	1.8270	-0.1470 ± 1.0628i	0
3	−90.3805	0.0192 ± 1.0301i	0

According to table 1, the equilibria set contain a number of saddle focal equilibria with index-1 or 2, which provides the possibility to generate chaos.

4. The chaotic circuit implementation

Modular design method is applied to obtain a chaotic circuit and a chaotic attractor is obtained by multisim simulation. The amplifier TL082 is used in this paper, whose power supply voltage is $V_{CC} = 15$ V, $V_{EE} = -15$ V. The whole circuit shown in figure 8 consists of four modules. Each module can implement a dimensionless equation in eq. (11). In the first module, the two amplifiers U1 and U2 are used to realize the function of integration and inversion, respectively. In the second module also, the two amplifiers U3 and U4 are used to realize the function of integration and inversion. In the third module, amplifier U5 is only used to implement the function of integration. In the last module, the variable x will be reversed and applied to the input of the amplifier U6, realizing the process of integration, and then the output from U6 would be applied to multiplication, amplification and inversion operation circuit in order to obtain the variable w^2 and $0.1w^4$. The whole circuit of the chaotic system is shown in figure 8 and the chaotic attractor is shown in figure 9.

The descriptions of U1, U3, U5, U6 in figure 8 are as follows:

$$\begin{cases} v_x = -\int \left[\dfrac{1}{R_1C_1} v_x - \dfrac{1}{R_2C_1} v_y - \dfrac{g_2}{R_4C_1} v_w^2 v_x \right. \\ \qquad \left. + \dfrac{g_1g_4}{R_3C_1} v_w^4 v_x \right] \mathrm{d}t \\ v_y = -\int \left[-\dfrac{1}{R_5C_2} v_x - \dfrac{1}{R_6C_2} v_y + \dfrac{1}{R_7C_2} v_z \right] \mathrm{d}t. \\ v_z = -\int \left[-\dfrac{1}{R_8C_3} v_y + \dfrac{1}{R_9C_3} v_z \right] \mathrm{d}t \\ v_w = -\int \left[-\dfrac{1}{R_{10}C_4} v_x \right] \mathrm{d}t \end{cases} \tag{20}$$

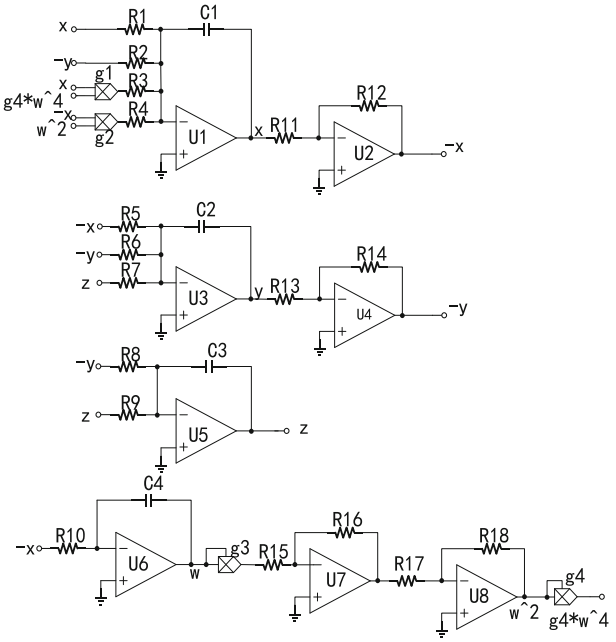

Figure 8. The three-scroll chaotic system circuit.

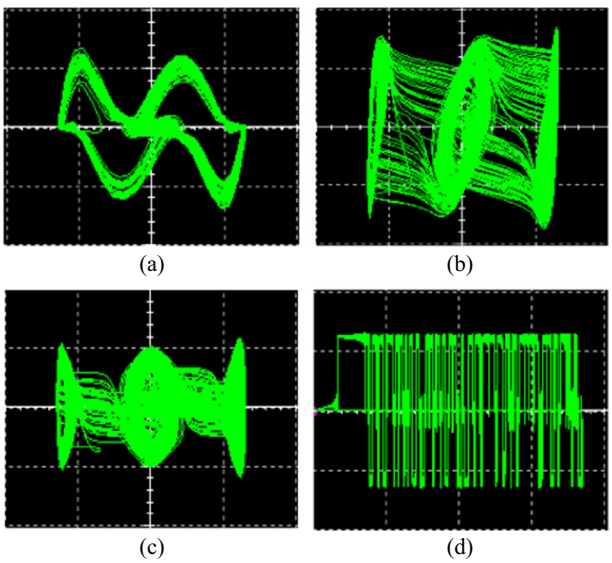

Figure 9. Chaotic attractor obtained by circuit simulation. (**a**) w–x plane, (**b**) w–y plane, (**c**) w–z plane and (**d**) time domain waveform of w.

Its differential equations:

$$\begin{cases} \dot{v}_x = -\dfrac{1}{R_1C_1}v_x + \dfrac{1}{R_2C_1}v_y \\ \qquad + \dfrac{g_2}{R_4C_1}v_w^2 v_x - \dfrac{g_1g_4}{R_3C_1}v_w^4 v_x \\ \dot{v}_y = \dfrac{1}{R_5C_2}v_x + \dfrac{1}{R_6C_2}v_y - \dfrac{1}{R_7C_2}v_z\,. \\ \dot{v}_z = \dfrac{1}{R_8C_3}v_y - \dfrac{1}{R_9C_3}v_z \\ \dot{v}_w = \dfrac{1}{R_{10}C_4}v_x \end{cases} \tag{21}$$

So we set $R_1 = 16.7\ \text{k}\Omega$, $R_2 = 13.3\ \text{k}\Omega$, $R_3 = 444\ \Omega$, $R_4 = 920\ \Omega$, $R_5 = 1587.3\ \text{k}\Omega$, $R_6 = 96.4\ \text{k}\Omega$, $R_8 = 47.6\ \text{k}\Omega$, $R_7 = R_9 = R_{10} = 100\ \text{k}\Omega$, $C_1 = C_2 = C_3 = C_4 = 100\ \text{nF}$ and $g_1 = g_2 = g_3 = g_4 = 0.1\ \text{V}^{-1}$, denoting the coefficient factor of the multiplier.

The circuit including amplifiers U2, U4 and U8 realizes reverse operation. The arithmetic unit U7 is used to implement amplification. So we can set $R_{11} = R_{12} = R_{13} = R_{14} = R_{15} = R_{17} = R_{18} = 1\ \text{k}\Omega$ and $R_{16} = 10\ \text{k}\Omega$.

Comparing the attractor shown in figure 9 with that in figure 5, we can conclude that the results of the numerical simulation agree with the results of the circuit experiment.

5. Conclusion

This paper proposes a new memristor-based multi-scroll hyperchaotic system, in which we can observe the complex chaotic phenomenon. Higher-order memductance are used in this chaotic system to increase complexity of the chaotic system. So we can generate a three-scroll chaotic attractor. Modular design method is applied to obtain a chaotic circuit, which is easy to implement. The dynamics of the proposed chaotic system is investigated, including the stability of the equilibrium points, the numerical simulations of bifurcation and Lyapunov exponents. Theoretical analysis, numerical simulation and circuit simulation results have confirmed the effectiveness of this approach.

Acknowledgements

This work is supported by the National Natural Science Foundation of China (No. 61571185), the Natural Science Foundation of Hunan Province, China (No. 2016JJ2030) and the Open Fund Project of Key Laboratory in Hunan Universities (No. 15K027).

References

[1] L O Chua, *IEEE Trans. Circuit Theory* **CT-18(5)**, 507 (1971)
[2] D B Strukov, *Nature* **453**, 80 (2008)
[3] M Itoh, *Int. J. Bifurcat. Chaos* **18(11)**, 3183 (2008)
[4] B Muthuswamy, *IETE Technical Rev.* **26(6)**, 415 (2009)
[5] B Muthuswamy, *Int. J. Bifurcat. Chaos* **20(5)**, 1335 (2010)
[6] B C Bao, *Chin. Phys. Lett.* **27(7)**, 070504 (2010)
[7] B C Bao, *Chin. Phys. B* **20(12)**, 120502 (2011)
[8] B C Bao, *Chin. Phys. B* **19(3)**, 030510 (2010)
[9] B C Bao, *Electron. Lett.* **46(3)**, 228 (2010)
[10] B C Bao, *Acta Phys. Sinica* **59(6)**, 3785 (2010)
[11] B C Bao, *Acta Phys. Sinica* **60(12)**, 120502 (2011)
[12] B C Bao, *Int. J. Bifurcat. Chaos* **21(9)**, 2629 (2011)

[13] Z J Li, *Chin. Phys. B* **22(4)**, 040502 (2013)
[14] F Corinto, *IEEE Trans. Circuits and Systems I*: *Regular Papers* **58(6)**, 1323 (2011)
[15] L D Wang, *Int. J. Bifurcat. Chaos* **22(8)**, 1250205 (2012)
[16] A Buscarino, *Chaos* **22(2)**, 023136 (2012)
[17] P Zhou, *Nonlinear Dyn.* **76**, 473 (2014)
[18] Q D Li, *Nonlinear Dyn.* **79**, 2295 (2015)
[19] H F Li, *Int. J. Bifurcat. Chaos* **24(7)**, 1450099 (2014)
[20] L Teng, *Nonlinear Dyn.* **77**, 231 (2014)
[21] Y N Joglekar, *Eur. J. Phys.* **30**, 661 (2009)